BOREAL ENVIRONMENT RESEARCH 22: 369–383
ISSN 1797-2469 (online)

Helsinki 14 September 2017

Fine-scale analysis of sea effect on coastal air temperatures at different time scales

Risto Väyrynen, Juuso Suomi* and Jukka Käyhkö

*Department of Geography and Geology, FI-20014 University of Turku, Finland (*corresponding author's e-mail: juuso.suomi@utu.fi)*

Received 24 Mar. 2017, final version received 10 Aug. 2017, accepted 8 Aug. 2017

Väyrynen R., Suomi J. & Käyhkö J. 2017: Fine-scale analysis of sea effect on coastal air temperatures at different time scales. *Boreal Env. Res.* 22: 369–383.

We analysed the effects of the Baltic Sea on coastal temperatures in the Turku region (SW Finland) using a six-year long data series from a network of 36 temperature loggers. The sea effect was filtered from other factors with monthly linear regression models for average, daily minimum and daily maximum temperatures. The sea effect (in °C) was determined using a variable combining the shortest distance to the shoreline and the area of waterbodies within a buffer zone. The sea effect proved to be the strongest in spring and in autumn. The sea effect caused an increase in daily minimum temperatures (warming effect). Daily average temperatures also increased in summer, autumn and winter due to the sea effect; in spring however, there no such increase was recorded. Based on multiple linear regression, the maximum absolute increase in temperatures due to the sea effect occurs during night in late summer and early autumn (by ca. 2 °C), while the maximum decrease occurs in daytime in spring and early summer (by ca. 0.7 °C).

Introduction

The vicinity of large waterbodies, such as sea or large lakes, is known to substantially affect climate at regional and local scales, as well as temporally during day and night, and in different seasons (*see* e.g. Wells 2012). A large waterbody moderates local temperature conditions typically by elevating mean minimum temperatures and by decreasing mean maximum temperatures. Climatologically, this is a well-known feature called maritime climate. The specific heat of water is considerably higher than and thermal response slower than those of soil or barren rocky surfaces. Therefore, more solar energy will be needed to warm up a layer of water than a respective layer of soil. Moreover, circulation and mixing in the waterbody transports heat deeper from the surface and thereby, a large volume of water is involved in heat exchange and storage. Typically, surface water down to 30 metres depth is actively involved in diurnal exchange of heat between the waterbody and the atmosphere (Oke 1987). Large proportion of the incoming energy on sea surface is transformed into latent heat in evaporation, while only a minor proportion remains as sensible heat elevating surface temperature. On dry land surfaces evaporation is smaller and a larger proportion of incoming energy is in sensible form. This elevates surface temperatures, which in turn elevate temperature of the overlaying air (e.g. Hertzman 1997, McClathey 2005). In cold climates, ice cover strongly reduces heat and moisture fluxes to the atmosphere. Along

Editor in charge of this article: Veli-Matti Kerminen

with snow cover, its impact on the global climate system is substantial, making it an important climate-modifying factor (e.g. Flanner *et al*. 2011, Riihelä *et al*. 2013).

It is quite surprising that the effect of waterbodies on coastal climates has not been extensively studied, especially at a local scale: e.g., Scott and Huff (1997), who studied the Great Lakes Basin in the USA, are among the very few who carried out their research in cool climates, resembling the conditions in our study area.

The Baltic Sea is a semi-closed, relatively shallow, brackish, inland sea that freezes partially during winter and is connected to the North Sea by Danish Straits (e.g. Mälkki and Tamsalu 1985). The phenomenon of maritimity and continentality in the Baltic Sea area was studied on at the regional scale by Laaksonen (1976, 1977) who used climatological data set covering the whole Baltic Sea basin.

In an attempt to quantify the effect of the sea on the climate of coastal areas, one has to identify and separate the effects of other factors such as land use. The urban heat island (UHI), i.e. elevated temperatures within a densely-built city relative to those in its rural surroundings, is an example of the land-use effect on local climate often most pronounced during nights with clear skies and weak winds. The main reasons for the existence of the UHI (*see* e.g. Oke 1987, Kłysik 1996, Arnfield 2003, Atkinson 2003) are (1) building materials that store and release solar energy in form of heat, (2) anthropogenic heat release from buildings and traffic, and (3) differences in evaporation between urban and non-urban areas. Examples of the numerical explanatory variables applied in UHI modelling are: surface albedo, aspect ratio, green density ratio, sky-view factor and average height-to-floor-area ratio (Giridharan *et al*. 2007, Kolokotroni and Giridharan 2008, Giridharan and Kolokotroni 2009). Various land-use data sets have proved useful in UHI research, as they often reflect thermal conditions of various urban land-use forms, and the results are easily extrapolated to larger scales (Hart and Sailor 2009, Szymanowski and Kryza 2012). Land-use data sets are cost-effective options as the availability of high-quality, open-source land-use data has been improved significantly during last years.

The effect of topography on spatial temperature variation depends on atmospheric stratification and topographic features of the area. During normal atmospheric conditions, temperature differences are substantial only in areas with variable topography. However, during stable atmospheric stratification, i.e. during inversions, temperature differences can be great even if the differences in elevation are small (Goldreich 1984, Pike *et al*. 2013). Consequently, a topographic variable, combining the effects of altitude (or relative elevation) with atmospheric stratification on temperature, should also be considered.

The effect of waterbodies on temperatures has been quantified with, e.g., distance to the nearest coastline (e.g. Eliasson and Svensson 2003) or the area of water inside a certain buffer zone (Steeneveld *et al*. 2011). Similarly to topography, also the type of the most appropriate variable for the effect of waterbody is case specific. Generally speaking, a distance-based variable is justifiable along coasts with only few islands and sharp land–water dichotomy, whereas a buffer zone variable may perform better in areas with a complex shoreline and a large archipelago (Suomi and Käyhkö 2012).

In addition to their separate effects, land use, topography and waterbodies often act together or affect each other in a complex manner. For example, depending on the season, proximity to large waterbodies can either strengthen or weaken the UHI intensity (Heino 1978, Suomi and Käyhkö 2012, Steeneveld *et al*. 2014). In certain cases, a waterbody can initiate the daytime urban cool island (e.g. Steinecke 1999, Gedzelman *et al*. 2003). In high-relief locations, natural barriers can emphasise coast–inland temperature differences caused by the sea (e.g. Tveito and Førland 1999). Deep and long valleys that are exposed to the sea, on the other hand, can reduce the above-mentioned differences (Daly *et al*. 2002).

The aims of our study were: (1) to quantify the seasonal and diurnal sea effect in the city of Turku (SW Finland), (2) in order to reach aim 1, to filter out and eliminate the effects of other environmental factors, such as topography, urban morphology and construction materials, on local climate in the study area, and (3) to resolve the timing of a seasonal shift in the direction of the sea effect from a warming one to a cooling one, and vice versa.

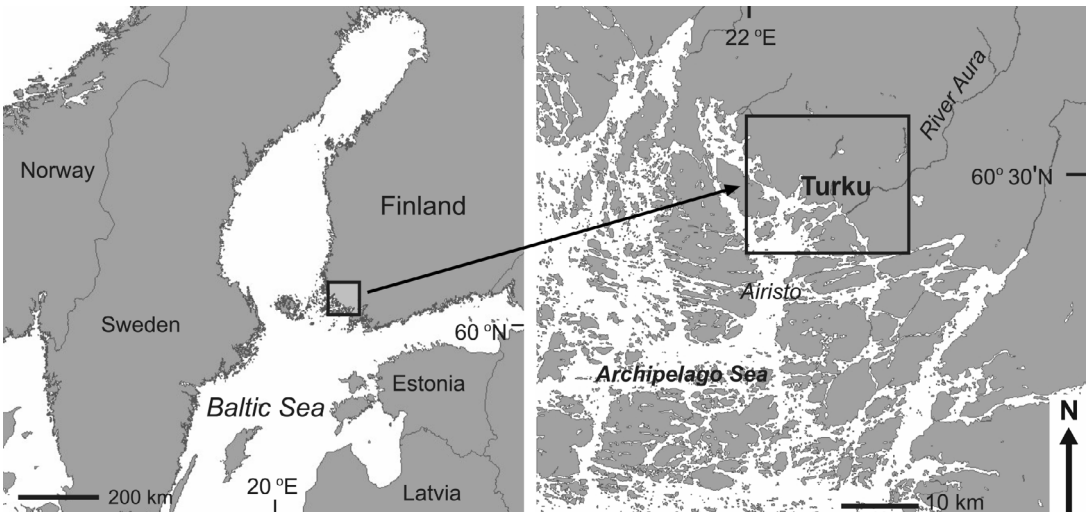

Fig. 1. The study area in SW Finland.

Study area

The study area (Fig. 1) consisted of a middle-size (186 000 inhabitants) coastal city of Turku and parts of its neighbouring municipalities. Turku (60°27´N, 22°16´E) is located in SW Finland at the mouth of the Aura river whose average discharge is 7 m^3 s^{-1}. The Baltic Sea coastline in the region is very complex with an archipelago of ca. 20 000 islands extending to the south-west. The shoreline within the Turku municipality is approx. 200 km long. The proportion of waterbodies inside the rectangular study area is 7%. Immediately off-shore the city centre are two islands: Ruissalo (9 km^2) and Hirvensalo (12 km^2). The nearest semi-open sea area is ~10 km south-west of the city centre. As a result, the climate of Turku is a combination of coastal and inland types. Depending on the movements of large weather systems, either continental or marine characteristics dominate (Huovila 1987).

In Köppen's climate classification, Turku belongs to the hemiboreal and humid continental Dfb class together with the southern parts of the Scandinavian Peninsula, the Baltic states and much of eastern Europe. The same climate type is found around the Great Lakes (USA) and at the mid-latitudes in western parts of Asia (Peel *et al*. 2007).

The annual (1981–2010) average temperature of the region is 5.5 °C based on the data from the weather station at the Turku airport 7 km to the north of the city centre. February is typically the coldest month, while July is the warmest, with average temperatures of –5.2 °C and 17.5 °C, respectively. The highest measured temperature in 1981–2010 was 32.1 °C (2010) and the lowest –34.8 °C (1987). The mean annual precipitation is 723 mm, of which 30% falls as snow. The average duration of permanent snow cover is approximately 90 days, starting from the second half of December. The wettest month is typically August (80 mm), while April is the driest (32 mm). Cyclonic activity brings about winds that are highly variable in speed and direction (average 3.4 m s^{-1}; dominant SW with a 17% proportion) (Pirinen *et al*. 2012; *see* also http://ilmasto-opas.fi/en/). With the annual average temperature of 6.0 °C, our study period 2002–2007 was 0.5 °C warmer than the 30-year climatic reference period 1981–2010. When considering monthly averages, only March and October in 2002–2007 were colder than average.

A distinctive factor in the climate of Turku is the spatio-temporal extent of the seasonal sea ice cover, which typically lasts for three months, starting approximately from the turn of the year. Depending on the seasonal weather conditions, the extent and timing may, however, vary considerably between the years (Seinä and Peltola 1991, Seinä *et al*. 2006). For example, during the winters 2001–2008, the annual maximum

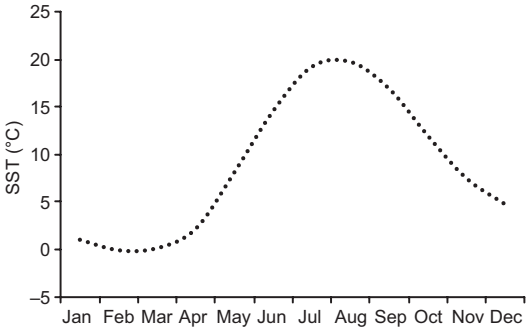

Fig. 2. Seasonal variation of sea surface temperature (SST) in the Turku area in 2002–2007.

ice cover proportion in the Baltic Sea varied between 12% and 58%, while the timing of the maximum ice extent stretched from 1 February to 24 March (*see* http://ilmatieteenlaitos.fi/jaatalvet [in Finnish]). As compared with ice-free conditions, continuous sea ice inhibits the thermal effect of the sea, bringing about continental climate. During the study period 2002–2007, the sea surface temperature in the study area varied between 0 and 20 °C (Fig. 2).

The Turku city centre has a spatial extent of 4 km (SW–NE) × 1.5 km (SE–NW) and is approximately rectangular. The street grid is oriented similarly, meaning that half of the streets are parallel to the dominant wind direction from SW. The market square is located in the middle of the city centre. Apartment and office 6–8-storey-high buildings with varying surface colours and materials as well as parks are the principal features in the area. The commercial areas are concentrated around the market square, while the rest of the area is residential. The Aura river (50–100 m wide) flows through the city centre. Industrial areas (docks, heavy/light industry) and retail parks lie scattered to the west and north of the city centre. The remaining areas are a mosaic of suburbs, forests and fields. The largest sparsely populated areas are found north of the city centre.

Topographically, the city area consists of flat clay ground 5–10 m a.s.l. with frequent, 30–50 m high bedrock outcrops. The hills host parks and are only partially covered with buildings. Outside the city centre, hills alternate with flat areas and the elevation rises gently inland, the highest places rising approx. 70 m a.s.l.

Material and methods

Temperature, land-cover and topographic data

The data we used in this study consist of temperature, land-use classification, and topography. Temperatures were measured by the Turku Urban Climate Research Group TURCLIM of the Department of Geography and Geology at the University of Turku. Altogether 36 Hobo H8 Pro temperature loggers with an uninterrupted observation period recorded temperature at 30-minute intervals in 2002–2007 (Fig. 3). The logger network is densest in the city centre, but the logger sites cover also rural, suburban and coastal areas and topographically varying locations (cf. Suomi *et al*. 2012). In our analyses we utilised monthly averages of daily minimum, daily maximum and average temperatures. The daily minimum and maximum values represent the lowest and highest temperatures, respectively, during a 24 hour day starting at 00:00 local solar time (GMT + 2). The manufacturer-declared accuracy of the instrument is ± 0.2 °C at 0–50 °C, while the resolution is 0.02 °C. Loggers are placed inside radiation shields on poles at 3-m elevation to minimise the risk of vandalism in densely populated areas.

To estimate the sea effect and eliminate the urban effect on temperatures, we used the SLICES land-use classification with the spatial resolution of 10 × 10 m and a total of 45 land-use classes, of which 42 were considered in our study area. SLICES is a national mapping project founded by the Ministry of Agriculture and Forestry and carried out by the National Land Survey of Finland (*see* http://citeseerx.ist.psu.edu/viewdoc/download?doi=10.1.1.201.8567&rep=rep1&type=pdf). The national digital elevation model (DEM) with a spatial resolution of 25 × 25 m was employed in estimating the effect of topography on spatio-temporal temperature variation.

Determining the urban effect

Of the original SLICES land-use classes, roads, office buildings, public buildings, and apartment buildings, positively affect temperatures in the

Fig. 3. Locations of the 36 temperature loggers (dots) that provided temperature data for the study. Loggers 1 (coast), 2 (city centre), and 3 (inland) were used in presenting the multiple linear regression results. The data from logger 3, which is located approx. 10 km NE of the city centre, were used also as a reference relative to which the sea effect was evaluated. Loggers 2 (city centre), 4 (coast) and 5 (inland) were used in examples (see text).

study area (Suomi and Käyhkö 2012), and they also represent typical urban land use forms. Consequently, we included those urban land-use classes in our multiple linear regression analysis.

Selection of an appropriate spatial scale is crucial in urban climate research. In earlier studies, many different buffer sizes extending from 15 m up to over 1 km were used (e.g. Giridharan *et al*. 2007, Giridharan and Kolokotroni 2009). For our study, we selected a circular buffer with the radius of 250 m, considering it large enough to include various urban environments and their direct and indirect effects on temperatures. This buffer size is in line with buffer sizes in earlier campaigns (*see* Suomi *et al*. 2012 and references therein).

To quantify urban heating (e.g., the UHI effect) the URB variable (i.e., the effective distance to the city centre) was defined as follows:

$$\mathrm{URB} = D_{\mathrm{city}} - U_{250} \times D_{\mathrm{city}}, \qquad (1)$$

where D_{city} is the actual distance to the city centre and U_{250} is the proportion of urban land-use classes inside the 250-m buffer zone around the logger.

The effective distance to the city centre decreases with increasing proportion of urban land-use types around the temperature observation point. In the case of near city-centre locations, the effective distance may increase if the proportion of urban land-use classes is locally reduced, e.g. in the vicinity of parks.

The resulting URB variable includes both large- and small-scale variation in urban heating. For example, relatively densely built suburbs located several kilometres away from the urban core, create small urban heat islands of their own. Also, urban parks and open areas appear as cool islands inside the warm city blocks.

Determining the sea effect

The effect of the sea decreases with increasing distance from the shoreline. Hence, to evaluate the sea effect, the logger located farthest away from the coastline (an arbitrary reference point; *see* Fig. 3: site 3) was selected as the one relative to which we calculated the differences in temperatures recorded by all other loggers. In

reality, the location of the reference point will not be constant, but will vary depending on the conditions. Subsequently, we introduced a SEA variable that included a distance component with the minimum, near-zero values being on the coast. We considered it necessary to include a buffer zone component in the SEA variable, as the coastline in the study area is extremely complex, and many islands are separated from the mainland only by narrow and shallow straits. We combined all water areas, such as inland lakes, rivers and sea areas as a single water area class, and calculated its proportion inside a circular buffer with the radius of 2000 m. Adjusting the buffer zone size to 2000 m for the SEA variable was based on the large thermal capacity and latent heat storage of waterbodies (*see* Suomi and Käyhkö 2012). The SEA variable (i.e., the effective distance to the shoreline from each temperature logger) was defined as follows:

$$\mathrm{SEA} = D_{\mathrm{shore}} - S_{2000} \times D_{\mathrm{shore}}, \quad (2)$$

where D_{shore} is the actual distance to the shoreline and S_{2000} is the proportion of waterbodies inside the 2000-m buffer zone around the logger. The theoretical point of maximum sea-effect, with continentality at its minimum, is located in the sea where there is only water within the 2-km buffer zone. Within our study area, the marine effect, defined by the variable SEA, was greatest at logger site 1 (Fig. 3). Consequently, logger site 1 was used, together with continental reference logger site 3 for demonstrating the regression-based sea effect in °C.

Determining the effects of topography

In our study area, differences in elevation are less than 70 m. Therefore, the relief-induced cold air pooling is more important topography-related local climatic phenomenon than the variation due to environmental lapse rate during normal atmospheric stratification (Suomi and Käyhkö 2012). The ground elevation rises smoothly towards the inland, which means that some of the inland valley bottoms lie at higher altitudes than hilltops by the coast. Therefore, relative elevation is more indicative than altitude as a topographic variable.

In relative elevation calculations, we used a circular buffer of 500 m in radius. Such size was based on our earlier experience and the topographic features of the study area.

The topographic variable that takes into account the relative elevation of each temperature measurement site is in multiple linear regression in the form

$$\mathrm{ELEV} = E_{\mathrm{location}} - E_{\mathrm{buffer500}}, \quad (3)$$

where E_{location} is the elevation (m a.s.l.) of temperature logger and $E_{\mathrm{buffer500}}$ is the average elevation of the buffer zone around the logger. In practice, the variable indicates whether the temperature-logger site is located lower or higher than the surroundings.

Multiple linear regression

In multiple linear regression analysis, we used as dependent variables the monthly averages of daily minimum, maximum and mean temperatures. Monthly values (instead of a shorter period) were used specifically to eliminate the effects of short-term weather variability on the results. Multicollinearity between the dependent variables was negligible. Our multiple linear regression is:

$$\mathrm{TEMP} = b_0 + b_1 \times \mathrm{SQRT(URB)} + b_2 \times \mathrm{SEA} + b_3 \times \mathrm{ELEV} \quad (4)$$

The sign of a regression coefficient indicates the warming or cooling effect of each variable. In case of URB, b_1 is negative when the temperature decreases when moving away from the city centre. The warming or cooling effect of the sea is expressed by the SEA variable and the sign of b_2 in the same way as in case the URB variable. For example, if a narrow on-shore zone is warmed by the sea, b_2 is negative. In case of topographic variable ELEV, positive b_3 means that relatively high-lying sites are warmer than relatively low-lying ones. If there is a change from a warming effect to a cooling one, or vice versa, also the sign of the respective regression coefficient (b) changes.

Case study periods

To demonstrate the variable sea effect in the study area, we made a seasonal comparison for two periods: late April with relatively cold sea water (spring), and late August with relatively warm seas (summer). In order to focus on seasonal rather than weather-driven differences, we selected similar south-westerly weather types for the comparison. The SW weather type is the dominating one in the study area, resulting in on-shore winds blowing from the sea towards the inland. Hence, it decreases the potential of diurnal sea/land breeze circulation. We used the temperature measurements from three loggers located at: site 4 on the coast (*see* Fig. 3), site 2 in the city centre (*see* Fig. 3), and site 5 inland (rural) several kilometres from the shore (*see* Fig. 3). The coastal and inland sites are rural in land use, and topographically rather similar so that temperature differences between them would reflect the pure sea effect only.

Results

Regression models

The explanatory power of the regression was the highest for average temperatures and the lowest for daily maximum temperatures. For monthly average temperatures, the adjusted R^2 values varied between 0.86 and 0.68, being the highest for March and April and the lowest for September (*see* Table 1 and Fig. 4). For maximum temperatures, R^2 values varied between 0.72 and 0.27, with the highest values for December and January and the lowest for September. For minimum temperatures, the highest R^2 value was 0.81 for February and the lowest 0.60 for October. Generally, the R^2 values were highest for late winter and spring, and lowest for summer and autumn.

In the model, the urban (URB) variable was always statistically significant (at $p = 0.05$) (Table 2). Its regression coefficient varied among months but was always negative indicating urban heating. Urban heating contributed the most to overall temperature increase in spring and summer, and the least in autumn and winter.

The SEA variable was statistically significant (at $p = 0.05$) for the majority of months. The exceptions were April, May and June for average temperatures and March and September for maximum temperatures (Table 2). The highest absolute β values of the SEA variable were found for autumn and winter. In case of the maximum temperatures, the sea causes cooling during spring and consequently, the highest maximum temperatures are measured far from the coastline. The warming effect is resumed in autumn. The cooling effect of the sea was mainly apparent in maximum temperatures. For minimum temperatures, the sea had a distinct warming effect throughout the year (Fig. 4).

The ELEV variable was statistically significant mainly in case of the minimum temperatures as well as in case of the maximum temperatures during autumn and winter. For the average temperatures, however, it was statistically significant in a few cases only.

Effect of the sea

Average temperatures

Average temperatures during most of the year were higher near the coastline than in more continental locations. In the study area, the temperature difference was approximately 1 °C during autumn and winter (Fig. 5). However, during April and May there was no difference in average temperatures between inland and coastal locations as near the coastline daytime cooling effect of the sea was cancelled out by its nighttime warming impact.

Maximum temperatures

Compared with the most continental measurement sites in the study area, proximity to the sea reduced maximum temperatures near the coastline in spring and early summer. The cooling effect of the sea was the strongest between April and June (as much as 0.7 °C) weakening gradually during late summer and early autumn (Figs. 6 and 7). The warming effect was the strongest between November and January, when

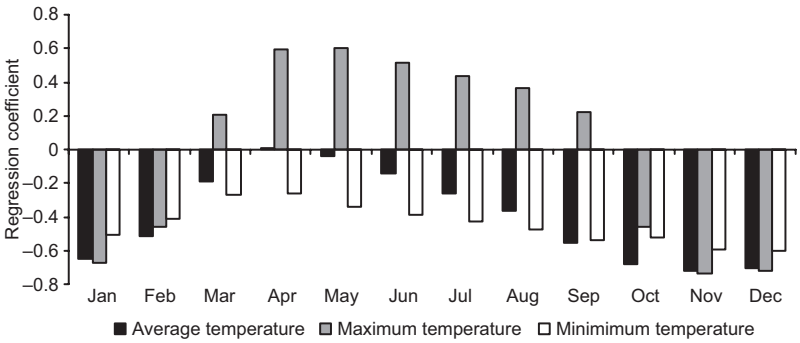

Fig. 4. Standardised regression coefficient of the SEA variable indicating warming (negative values) or cooling (positive values) effect of the sea as compared with logger 3 location (*see* Fig. 3).

maximum temperatures near the coastline were as much as 0.8 °C higher than those in the inland locations. The shift from the autumn–winter warming effect of the sea to the spring–summer time cooling one happened around the turn of February and March, and from cooling to warming around the turn of September and October.

Minimum temperatures

According to the regression, the effect of the sea is warming one throughout the year. The greatest temperature difference occurred in late summer (August–September), when the minimum temperatures were almost 2 °C higher near the coastline than at the inland reference point (Figs. 7 and 8). Temperature difference between the coastal and inland locations was the smallest (ca. 0.7 °C) in April.

Examples

The sea effect on temperatures was noticeable during the one-week case study periods. In spring (late April 2002), the sea surface temperatures were relatively low after the winter, winds weak and skies partly clear, especially during nights. The warming effect of the sea was relatively small, but noticeable (Fig. 9). The daytime cooling effect was relatively strong, being almost 5 °C. The city-centre measurement point (logger 2) was usually the warmest during night. At the inland location (logger 5) where the night-time minimum temperatures were low, the daytime temperatures were high. At both the inland and coastal points (loggers 5 and 4, respectively) relief-induced cool-air ponds tended to develop at night.

In early autumn (August–September 2002), temperature differences between the city centre

Table 1. Monthly R^2 and adjusted R^2 values of the linear regression models for average, daily maximum and daily minimum temperatures.

	Average *T*		Maximum *T*		Minimum *T*	
	R^2	adj. R^2	R^2	adj. R^2	R^2	adj. R^2
January	0.824	0.808	0.743	0.719	0.785	0.765
February	0.854	0.840	0.642	0.608	0.825	0.808
March	0.872	0.860	0.461	0.411	0.810	0.792
April	0.871	0.859	0.519	0.474	0.792	0.773
May	0.844	0.829	0.496	0.449	0.747	0.724
June	0.775	0.754	0.459	0.408	0.723	0.697
July	0.759	0.736	0.462	0.412	0.717	0.691
August	0.738	0.713	0.421	0.367	0.715	0.688
September	0.702	0.675	0.329	0.266	0.687	0.658
October	0.710	0.683	0.493	0.445	0.637	0.602
November	0.766	0.744	0.739	0.714	0.698	0.669
December	0.781	0.761	0.745	0.721	0.756	0.733

(logger 2) and the coastal location (logger 4) were smaller (Fig. 10). The daytime cooling effect of the sea was smaller than in the spring-, while the night-time warming effect was much stronger due to the higher sea surface temperatures. Night-time temperatures at the inland location (logger 5) were remarkably low and the temperature difference between coastal and inland locations reached 8 °C. However, this period was slightly cloudier than the one in the spring, which may explain some of the temperature features.

Discussion

We used the data from a dense temperature measurement network to quantify the spatio-

Table 2. Standardised regression coefficients (β) and respective statistical significance of each variable in multiple linear regressions for monthly average, maximum and minimum temperatures.

	SQRT URB		SEA		ELEV	
	β_1	p	β_2	p	β_3	p
Average *T*						
January	–0.473	< 0.001	–0.647	< 0.001	0.028	0.711
February	–0.625	< 0.001	–0.516	< 0.001	0.045	0.510
March	–0.827	< 0.001	–0.188	0.008	0.170	0.012
April	–0.922	< 0.001	0.011	0.865	0.097	0.138
May	–0.901	< 0.001	–0.036	0.623	0.049	0.489
June	–0.823	< 0.001	–0.140	0.122	0.052	0.546
July	–0.756	< 0.001	–0.256	0.008	0.045	0.607
August	–0.665	< 0.001	–0.362	0.001	0.094	0.312
September	–0.475	< 0.001	–0.555	< 0.001	0.065	0.507
October	–0.336	0.002	–0.676	< 0.001	0.040	0.680
November	–0.340	0.001	–0.721	< 0.001	–0.062	0.478
December	–0.376	< 0.001	–0.704	< 0.001	–0.041	0.625
Maximum *T*						
January	–0.371	< 0.001	–0.669	< 0.001	–0.276	0.005
February	–0.484	< 0.001	–0.455	< 0.001	–0.385	0.001
March	–0.652	< 0.001	0.203	0.144	–0.309	0.024
April	–0.581	< 0.001	0.596	< 0.001	–0.146	0.247
May	–0.578	< 0.001	0.599	< 0.001	–0.035	0.782
June	–0.612	< 0.001	0.514	0.001	–0.007	0.955
July	–0.661	< 0.001	0.436	0.003	–0.038	0.772
August	–0.630	< 0.001	0.363	0.015	–0.176	0.204
September	–0.494	0.003	0.224	0.149	–0.338	0.027
October	–0.324	0.019	–0.454	0.002	–0.404	0.003
November	–0.269	0.008	–0.735	< 0.001	–0.260	0.007
December	–0.304	0.003	–0.718	< 0.001	–0.261	0.007
Minimum *T*						
January	–0.498	< 0.001	–0.503	< 0.001	0.287	0.002
February	–0.620	< 0.001	–0.406	< 0.001	0.273	0.001
March	–0.675	< 0.001	–0.268	0.002	0.339	< 0.001
April	–0.694	< 0.001	–0.260	0.004	0.291	0.001
May	–0.639	< 0.001	–0.338	0.001	0.236	0.013
June	–0.581	< 0.001	–0.387	< 0.001	0.245	0.013
July	–0.550	< 0.001	–0.427	< 0.001	0.230	0.021
August	–0.479	< 0.001	–0.473	< 0.001	0.279	0.006
September	–0.371	0.001	–0.539	< 0.001	0.299	0.005
October	–0.335	0.005	–0.518	< 0.001	0.317	0.006
November	–0.383	0.001	–0.588	< 0.001	0.194	0.056
December	–0.418	< 0.001	–0.596	< 0.001	0.204	0.027

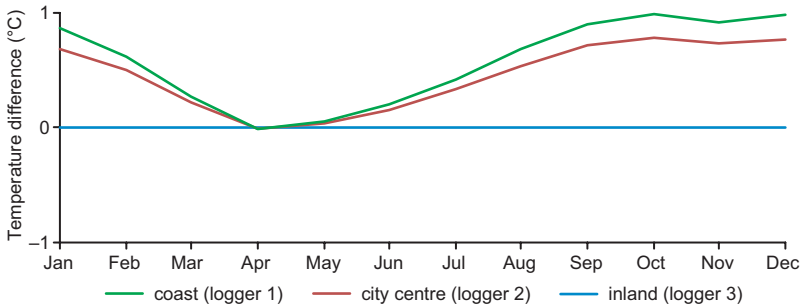

Fig. 5. Differences in modelled monthly average temperatures between the coast and city centre, and the reference point (inland). For logger locations *see* Fig. 3.

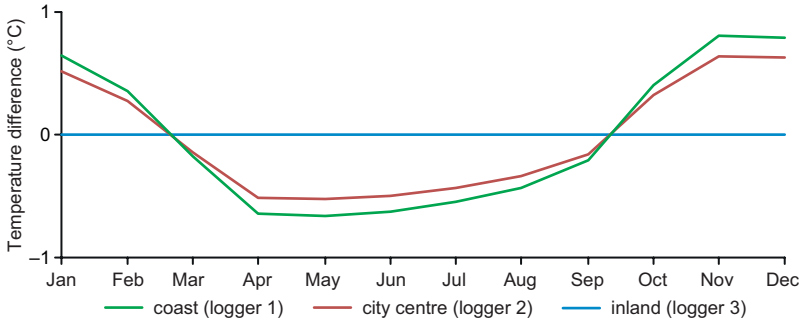

Fig. 6. Differences in modelled monthly maximum temperatures between the coast and city centre, and the reference point (inland). For logger locations *see* Fig. 3.

temporal effect of sea on the climate of a high-latitude coastal town. Multiple linear regression with three area and distance based variables (SEA, URB and ELEV) managed to explain well the differences in monthly average and minimum temperatures in the study area. For monthly maximum temperatures, the explanatory power of the regression was lower. The most apparent sea effect in the study area was the seasonal shift from spring cooling to autumn and early-winter warming. Similar results were also obtained by Laaksonen (1976, 1977).

In case of the daily minimum temperatures, warming was evident throughout the year. For daily maximum temperatures, cooling dominated in spring, while warming in autumn and early winter. For average temperatures, the sea had a warming effect for most of the year, only April and May were rather neutral. Our results support the earlier observations of Suomi and Käyhkö (2012) who investigated the effects of environmental factors on spatial temperature differences in the same region with a buffer-based model setting.

Eliasson and Svensson (2003) concluded that temperature variations are generally more dependent on weather conditions than season. This was also observed by Hjort *et al*. (2011), who stated that predominant weather conditions, such as cloudiness and high winds, overrule local geographical factors more frequently during autumn and winter which complicates the spatial modelling. This conclusion is partly supported also by our regression analysis results: R^2 values were the lowest in summer and autumn. According to Svensson *et al*. (2002) and Eliasson and Svensson (2003) in the city of Gothenburg on the Swedish west coast, the distance from the sea is an important factor explaining variability in temperatures not only during cloudy and windy but also during calm and clear conditions. Aikawa *et al*. (2007) reported similar results from Japan. They concluded that in August, the highest temperatures occur generally within 5–10 km from the coast, while in December, on the coast itself. Svensson *et al*. (2002) pointed out that when the distance to the sea increases, the wind speed in open areas decreases exponentially. Also in

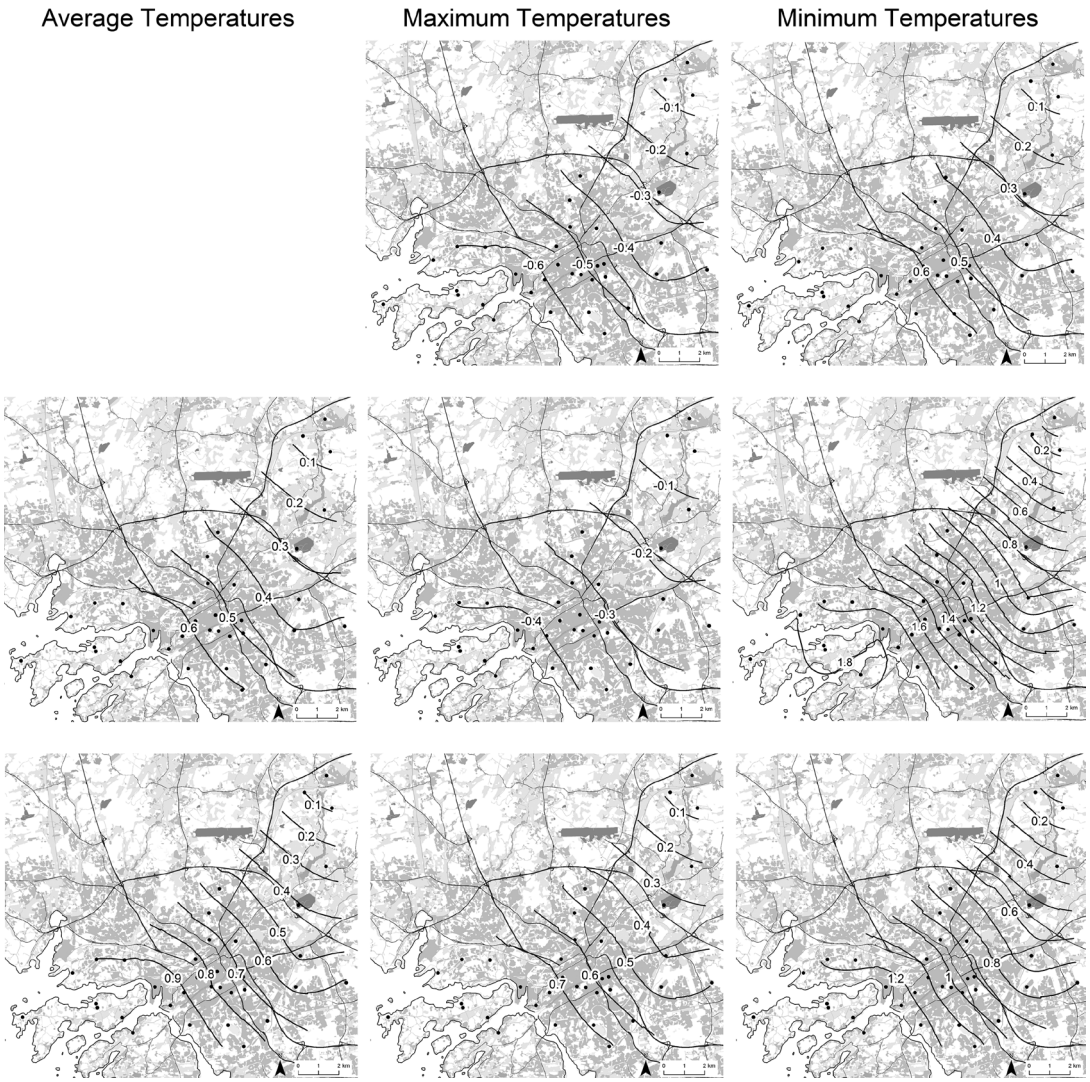

Fig. 7. The modelled cooling/warming effects of the sea in °C in April (**a**–**b**), August (**c**–**e**) and December (**f**–**h**). In April, the variation in average temperatures was below 0.1 °C and hence, the first image is not included.

our study, part of the warming effect of the sea could be explained by stronger winds near the coastline, where mixing of the air breaks the surface inversion layers. Ice-free water also provides moisture that turns into low clouds during cold winter. In addition, moisture elevates the dew-point temperature which in turn affects the nocturnal minimum temperature.

The narrow and relatively shallow sounds and straits between many islands that are a distinctive feature of SW Finland partly prevent and complicate land–sea wind circulation as compared with sites with steeper land–sea dichotomy. As the preconditions for land–sea breeze circulation in the area are most favourable during spring and early summer, when the temperature difference between sea and land is the greatest, the land–sea breeze circulation probably plays a role in the fact that the standardised regression coefficient values indicating daytime cooling effect of the sea were greatest in April, May and June.

As per the effect of the URB and ELEV variables on temperature, the URB effect was strong

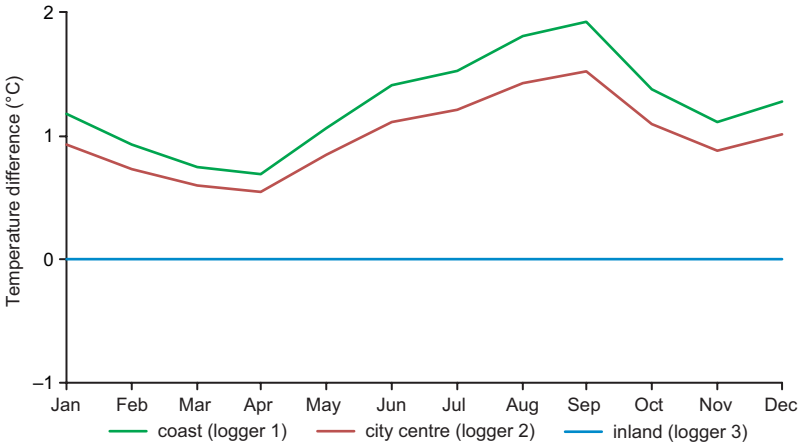

Fig. 8. Differences in modelled monthly minimum temperatures between the coast and city centre, and the reference point (inland). For logger locations *see* Fig. 3.

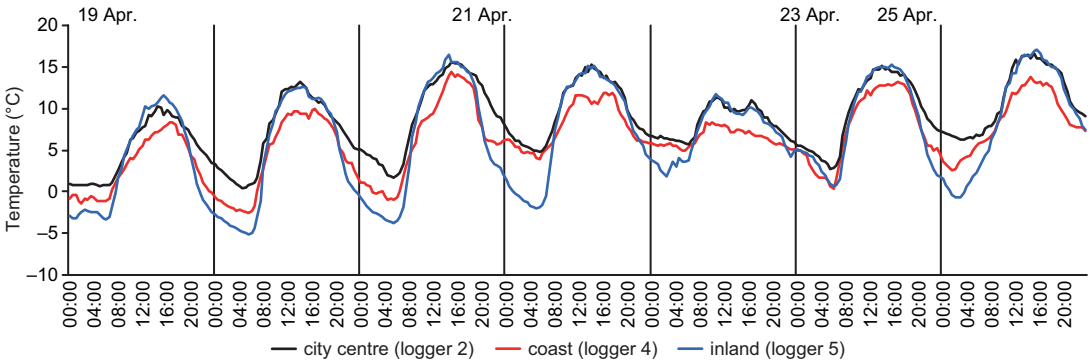

Fig. 9. Temperatures measured at selected sites in spring 2002 during SW weather type, when water temperatures were relatively low compared with the air temperatures. For logger locations *see* Fig. 3.

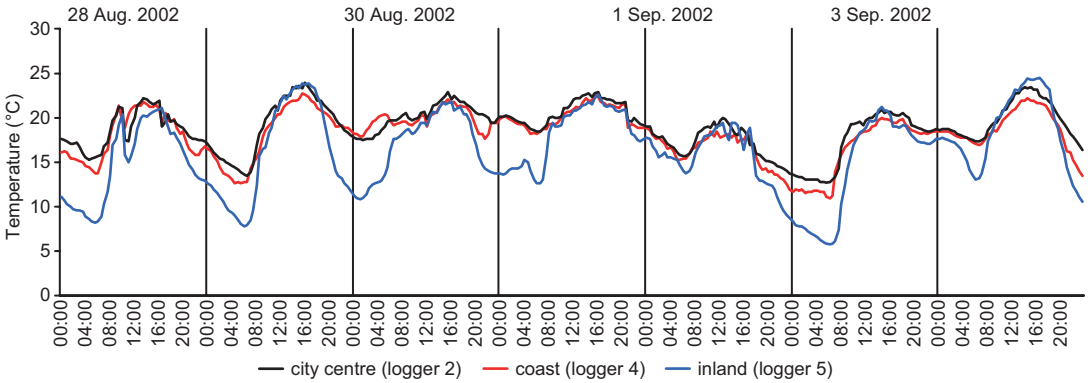

Fig. 10. Temperatures measured at selected sites in early autumn 2002 during SW weather type, when water temperatures were relative high compared to the air temperatures. For logger locations *see* Fig. 3.

and always a warming one, while that of ELEV was clearly the weakest. Topography (ELEV) affected temperatures mainly through nocturnal cold-air pooling.

When strong urban heat islands (UHI) develop, they can substantially modify the effect of the sea on local temperatures (Freitas *et al.* 2007, Suomi 2014). The interaction between

urban and sea effects was identified at high latitudes also by e.g. Steinecke (1999) in Reykjavik, Iceland, where the cooling effect of the nearby Atlantic Ocean produced an urban cold island in the city centre in summer, a phenomenon that was also observed in our study area by Suomi (2014).

The combined effect of sea (SEA) and topography (ELEV) was rather small as our study area is rather flat. This holds true despite the fact that the Aura river valley, being parallel to the prevailing wind direction from SW to NE, is likely to promote movement of marine air masses inland. Furthermore, the seasonal ice-cover and the relatively small volume of seawater in the Archipelago Sea and the whole Baltic Sea suppress the combined effect of topography (ELEV) and sea (SEA) on temperatures the SW Finland (cf. Daly *et al*. 2002).

Considering the climate warming and the potential need to increase UHI mitigation in the future, waterbodies have been proposed as means to lessen the UHI-driven heat accumulation (e.g. Krüger and Pearlmutter 2008, Coutts *et al*. 2013). Based on our observations, this may not always work. In our study area, the night-time heat surplus near open waterbodies may actually strengthen the night-time UHI intensity. A similar pattern was demonstrated by Steeneveld *et al*. (2014) in Rotterdam, Netherlands. Also Manteghi *et al*. (2015) discussed potential shortcomings of waterbodies as means of UHI mitigation.

As we used long-time average temperatures in our regression analysis, the climatic effect of sea ice could not be separated from the overall effect of the sea. It is likely that sea ice affects on temperatures not only locally near the coastline, but also throughout our study area. Snow covered and frozen sea areas have a higher albedo than land areas. This becomes evident in spring, when increasing solar radiation rises temperatures in darker land areas, while they remain lower above the frozen sea. This provides some extra cooling as compared with that of cold but open water (e.g. Laaksonen 1977). Also melting of snow and ice, and the following evaporative cooling reduces daytime temperatures near the coasts. The sea ice affects the atmospheric boundary layer and heat fluxes between ice and atmosphere (Brümmer *et al*. 2005). The effect of frozen sea is incorporated in our regression, but the exact distinction of what proportion of the thermal effect is attributed to frozen seas is an interesting future research topic.

The effect of the sea occasionally extended further inland than the most continental observation point (logger 3) in this study. Correspondingly, the maximum sea effect is observed in the outer archipelago outside the study area. Hence, the maximum heating and cooling effects of the sea are in reality somewhat greater than observed in this study area.

Rather high R^2 values, small differences between modelled and measured temperatures and comparisons with earlier studies carried out in the same area (Hjort *et al*. 2011, Suomi and Käyhkö 2012) indicate that a combination of distance- and buffer-zone-based variables is a good alternative for purely buffer-based model settings.

Conclusions

1. For daily minimum temperatures, the sea effect is always a warming one.
2. For average temperatures, the sea effect is mainly a warming one, except in spring, when it is rather neutral.
3. For daily maximum temperatures, the sea effect is twofold; the shift from warming in the cold season to cooling in the warm season takes place at the turn of February and March, and the turn of September and October, respectively.
4. The absolute and relative cooling effects of the sea is at its maximum during daytime in spring and early summer; it is approximately –0.7 °C when other factors (URB and ELEV) are eliminated.
5. The absolute warming effect of sea is at its maximum during night-time in late summer and early autumn; it is approximately +2 °C when other factors (URB and ELEV) are eliminated. The maximum relative sea effect is observed in late autumn and early winter.

Acknowledgements: The TURCLIM project collaborates with the Turku Environment and City Planning Department, whose assistance is highly appreciated. The long-term refer-

ence weather data were provided by the Finnish Meteorological Institute. We thank two anonymous reviewers for the valuable comments that helped to improve the manuscript.

References

Aikawa M., Hiraki T., Eiho J. & Miyazaki H. 2007. Characteristic air temperature distributions observed in summer and winter in urban area in Japan. *Environmental Monitoring and Assessment* 131: 255–265.

Arnfield A.J. 2003. Two decades of urban climate research: a review of turbulence, exchanges of energy and water, and the urban heat island. *International Journal of Climatology* 23: 1–26.

Atkinson B.W. 2003. Numerical modelling on urban heat-island intensity. *Boundary-Layer Meteorology* 109: 285–310.

Brümmer B., Kirchgässner A. & Müller G. 2005. The atmospheric boundary layer over Baltic Sea ice. *Boundary-Layer Meteorology* 117: 91–109.

Coutts A.M., Tapper N.J., Beringer J., Loughnan M. & Demuzere M. 2013. Watering our cities: the capacity for water sensitive urban design to support urban cooling and improve human thermal comfort in the Australian context. *Progress in Physical Geography* 37: 2–28.

Daly C., Gibson W.P., Taylor G.H., Johnson G.L. & Pasteris P. 2002. A knowledge-based approach to the statistical mapping of climate. *Climate Research* 22: 99–113.

Eliasson I. & Svensson M.K. 2003. Spatial air temperature variations and urban land use — a statistical approach. *Meteorological Applications* 10: 135–149.

Flanner M.G., Shell K.M., Barlage M., Perovich D.K. & Tschudi M.A. 2011. Radiative forcing and albedo feedback from the northern hemisphere cryosphere between 1979 and 2008. *Nature Geoscience* 4: 151–155.

Freitas D.E., Rozoff C.M., Cotton W.R. & Dias P.L.S. 2007. Interactions of an urban heat island and sea-breeze circulations during winter over the metropolitan area of São Paulo, Brazil. *Boundary Layer Meteorology* 122: 43–65.

Gedzelman S.D., Austin S., Cermak R., Stefano N., Partridge S., Quesenberry. S. & Robinson D.A. 2003. Mesoscale aspects of the urban heat island around New York City. *Theoretical and Applied Climatology* 79: 29–42.

Giridharan R. & Kolokotroni M. 2009. Urban heat island characteristics in London during winter. *Solar Energy* 83: 1668–1682.

Giridharan R., Lau S.S.Y., Ganesan S. & Givoni B. 2007. Urban design factors influencing heat island intensity in high-rise high-density environments of Hong Kong. *Building and Environment* 42: 3669–3684.

Goldreich Y. 1984. Urban topoclimatology. *Progress in Physical Geography* 8: 336–364.

Heino R. 1978. Urban effect on climatic elements in Finland. *Geophysica* 15: 171–187.

Hart M.A. & Sailor D.J. 2009. Quantifying the influence of land-use and surface characteristics on spatial variability in the urban heat island. *Theoretical and Applied Climatology* 95: 397–406.

Hertzman O. 1997. Oceans and the coastal zone. In: Bailey W.G., Oke T.R. & Rouse W.R. (eds.), *The surface climates of Canada*, McGill-Queen's University Press, Montreal & Kingston, pp. 101–123.

Hjort J., Suomi J. & Käyhkö J. 2011. Spatial prediction of urban–rural temperatures using statistical methods. *Theoretical and Applied Climatology* 106: 139–152.

Huovila S. 1987. Pienilmasto (Microclimate). In: Alalammi P. (ed.), *Atlas of Finland* 131, Maanmittaushallitus, Helsinki, pp. 23–26.

Kłysik K. 1996. Spatial and seasonal distribution of anthropogenic heat emissions in Lodz, Poland. *Atmospheric Environment* 30: 3397–3404.

Kolokotroni M. & Giridharan R. 2008. Urban heat island intensity in London: an investigation of impact of physical characteristics on changes in outdoor air temperature during summer. *Solar Energy* 82: 986–998.

Krüger E. & Pearlmutter D. 2008. The effect of urban evaporation on building energy demand in an arid environment. *Energy and buildings* 40: 2090–2098.

Laaksonen K. 1976. Factors affecting mean air temperatures in Fennoscandia. October and January 1920–1950. *Fennia* 145: 1–94.

Laaksonen K. 1977. The influence of sea areas upon mean air temperatures in Fennoscandia (1920–1950). *Fennia* 151: 57–128.

Manteghi G., Bin Limit H. & Remaz H. 2015. Water bodies an urban microclimate: a review. *Modern Applied Science* 9: 1–12.

McClathey J. 2005. Regional and local climates. In: Holden J. (ed.), *An introduction to physical geography and environment*, Pearson Education, Harlow, pp. 80–96.

Mälkki P. & Tamsalu R. 1985. *Physical features of the Baltic Sea*. Finnish Marine Research 252.

Oke T.R. 1987. *Boundary layer climates*, 2nd ed. Routledge, London and New York.

Peel M.C., Finlayson B.M. & McMahon T.A. 2007. Updated world map of the Köppen-Geiger climate classification. *Hydrology and Earth System Sciences* 11: 1633–1644.

Pike G., Pepin N.C., Schaefer M. 2013. High latitude local scale temperature complexity: the example of Kevo Valley, Finnish Lapland. *International Journal of Climatology* 33: 2050–2067.

Pirinen P., Simola S., Aalto J., Kaukoranta J-P., Karlsson P. & Ruuhela R. 2012. *Tilastoja Suomen ilmastosta 1981–2010*. Finnish Meteorological Institute, Helsinki. [Available at https://helda.helsinki.fi/bitstream/handle/10138/35880/Tilastoja_Suomen_ilmastosta_1981_2010.pdf?sequence=4].

Riihelä A., Manninen T. & Laine V. 2013. Observed changes in the albedo of the Arctic sea-ice zone for the period 1982–2009. *Nature Climate Change* 3: 895–898.

Scott R.W. & Huff F.A. 1997. *Lake effects on climatic conditions in the Great Lakes Basin*. Contract Report 617 (MCC Research Report 97-01), Illinois State Water Survey Champaign, IL. [Available at http://www.isws.illinois.edu/pubdoc/CR/ISWSCR-617.pdf].

Seinä A. & Peltola J. 1991. Duration of the ice season and statistics of fast ice thickness along the Finnish coast 1961–1990. *Finnish Marine Research* 258: 1–46.

Seinä A., Eriksson P., Kalliosaari S. & Vainio J. 2006. Ice seasons 2001–2005 in Finnish sea areas. *Report Series of the Finnish Institute of Marine Research* 57: 1–94.

Steeneveld G.J., Koopmans S., Heusinkveld B.G. & Theeuwes N.E. 2014. Refreshing the role of open water surfaces on mitigating the maximum urban heat island effect. *Landscape and Urban Planning* 121: 92–96.

Steeneveld G.J., Koopmans S., Heusinkveld B.G., van Hove L.W.A. & Holtslag A.A.M. 2011. Quantifying urban heat island effects and human comfort for cities of variable size and urban morphology in the Netherlands. *Journal of Geophysical Research* 116: 92–96.

Steinecke K. 1999. Urban climatological studies in Reykjavik subarctic environment. Iceland. *Atmospheric Environment* 33: 4157–4162.

Suomi J. 2014. *Characteristics of urban heat island (UHI) in a high-latitude coastal city - a case study of Turku, SW Finland*. Ph.D. thesis, Department of Geography and Geology, University of Turku.

Suomi J., Hjort. J. & Käyhkö J. 2012. Effects of scale on modelling the urban heat island in Turku. SW Finland. *Climate Research* 55: 105–118.

Suomi J. & Käyhkö J. 2012. The impact of environmental factors on urban temperature variability in the coastal city of Turku, SW Finland. *International Journal of Climatology* 32: 451–463.

Svensson M.K., Eliasson I. & Holmer B. 2002. A GIS based empirical model to simulate air temperature variations in the Göteborg urban area during the night. *Climate Research* 22: 215–226.

Szymanowski M. & Kryza M. 2012. Local regression models for spatial interpolation of urban heat island - an example from Wrocław, SW Poland. *Theoretical and Applied Climatology* 108: 53–71.

Tveito O.E. & Førland E.J. 1999. Mapping temperatures in Norway applying terrain information, geostatistics and GIS. *Norsk Geografisk Tidsskrift — Norwegian Journal of Geography* 53: 202–212.

Wells N. 2012. *The atmosphere and ocean — a physical introduction*, 3rd ed. John Wiley-Blackwell, Chichester.